A Presenilin-2–ARF4 trafficking axis modulates Notch signaling during epidermal differentiation

Ellen J. Ezratty, H. Amalia Pasolli, and Elaine Fuchs

Howard Hughes Medical Institute, Robin Chemers Neustein Laboratory of Mammalian Cell Biology and Development, The Rockefeller University, New York, NY 10065

How primary cilia impact epidermal growth and differentiation during embryogenesis is poorly understood. Here, we show that during skin development, Notch signaling occurs within the ciliated, differentiating cells of the first few suprabasal epidermal layers. Moreover, both Notch signaling and cilia disappear in the upper layers, where key ciliary proteins distribute to cell–cell borders. Extending this correlation, we find that Presenilin-2 localizes to basal bodies/cilia through a conserved VxPx motif. When this motif is mutated, a GFP-tagged Presenilin-2 still localizes to intercellular borders, but basal body localization is lost. Notably, in contrast to wild type, this mutant fails to rescue epidermal differentiation defects seen upon *Psen1* and *2* knockdown. Screening components implicated in ciliary targeting and polarized exocytosis, we provide evidence that the small GTPase ARF4 is required for Presenilin basal body localization, Notch signaling, and subsequent epidermal differentiation. Collectively, our findings raise the possibility that ARF4-dependent polarized exocytosis acts through the basal body–ciliary complex to spatially regulate Notch signaling during epidermal differentiation.

Introduction

One fundamental question in developmental biology is how an individual cell may sense its environment to transmit extracellular signals that control cell signaling and proliferation during tissue morphogenesis. Once thought merely a vestigial structure, the primary cilium is now well established as a cell-sensory organelle that coordinates signal transduction pathways (Berbari et al., 2009). Although cilia have been most prominently linked to Sonic Hedgehog (SHH) signaling, their appreciation as cellular "antennae" that sense a wide variety of external signals likely explains why ciliary defects contribute to diverse human disorders and diseases, such as polydactyly, neural tube defects, Bardet–Biedl syndrome, retinal degeneration, polycystic kidney disease, and skin cancer (Badano et al., 2006; Satir and Christensen, 2007).

In response to external environmental cues during skin embryogenesis, ciliated epithelial progenitors within a single (basal) layer either stratify and differentiate to generate the epidermis or invaginate to make the buds that will develop into hair follicles (HFs; Fuchs, 2007; Ezratty et al., 2011). Hair bud formation requires Wnt and Shh signaling (Ouspenskaia et al., 2016), and given the cilium's prominent role in Shh signaling, it is not surprising that primary cilia have a role in HF development (Ezratty et al., 2011). However,

defects in ciliogenesis also cause a temporally and spatially distinct perturbations in epidermal differentiation (Croyle et al., 2011; Ezratty et al., 2011), a process thought to occur independently of Shh signaling (Mill et al., 2005), but require Notch-signaling (Rangarajan et al., 2001; Lefort and Dotto, 2004; Blanpain et al., 2006). The role of the cilium in this latter process remains poorly understood.

Notch signaling is activated when one of four (Notch 1–4) Notch receptors engages with Delta or Jagged ligands, typically presented on an adjacent neighboring cell. Upon ligand activation, Notch receptors are cleaved in a cascade of proteolytic events, culminating in Presenilin-mediated enzymatic cleavage and subsequent release of the Notch intracellular domain (NICD). NICD then translocates to the nucleus and associates with the DNA-binding protein RBPj to activate downstream target genes that are required for differentiation (Kopan, 2012; Hori et al., 2013). When *Rbpj* is conditionally ablated in the basal layer of embryonic epidermis, Notch signaling is abrogated and epidermal differentiation is impaired, but cilia are unaffected (Blanpain et al., 2006; Ezratty et al., 2011). This places ciliogenesis upstream of Notch signaling in embryonic skin.

When *Ift88* is ablated postnatally in skin, the epidermis displays hyperproliferation and discontinuous keratin 1 (K1), suggestive of suppressed terminal differentiation (Croyle et al., 2011). Similarly, when *Ift88* or several other
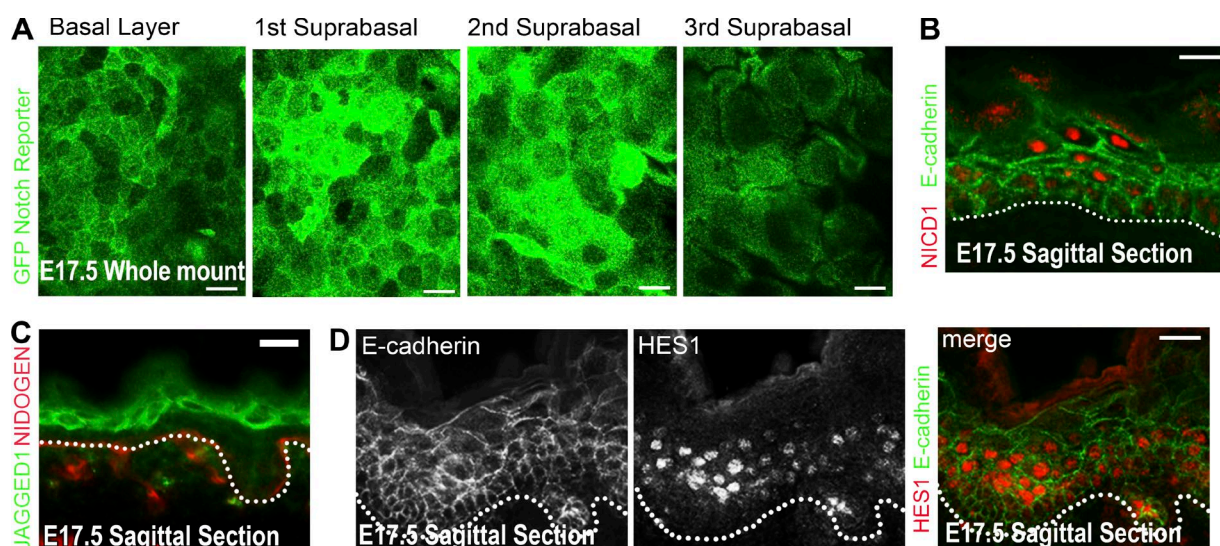
Figure 1. **Notch signaling is spatially activated within differentiating embryonic epidermis.** (A) Confocal images of basal or suprabasal planes from WM E17.5 epidermis isolated from TNR-GFP mouse. Green, GFP; blue, DAPI. (B) Sagittal section of E17.5 epidermis immunolabeled with antibody against Notch 1 intracellular domain (NICD1). (C) Sagittal section of E17.5 epidermis immunolabeled with antibodies against Notch ligand Jagged 1 (green) and basement membrane glycoprotein NIDOGEN (red). (D) Sagittal section of E17.5 epidermis immunolabeled with antibodies against E-cadherin (green) and HES1 (red). Dotted line denotes dermal–epidermal border. Bars: (A) 15 µm; (B–D) 30 µm.

Ift mRNAs are knocked down in embryonic skin by in utero, epidermal-specific delivery of lentiviruses harboring one of several different ciliary hairpin shRNAs, the epidermis displays hyperproliferation and diminished differentiation (Ezratty et al., 2011). Moreover, *Ift* mutant embryonic skin was accompanied by a reduction in canonical Notch reporter activity and nuclear pathway members NICD and HES1 (Ezratty et al., 2011). Given that ciliogenesis occurs before and independently of canonical Notch signaling, and epidermal ciliary mutants are defective in Notch-dependent epidermal differentiation, we became curious as to whether primary cilia may play a context-specific role in spatially and/or temporally regulating aspects of Notch signaling during embryogenesis.

In the present study, we sought to test the hypothesis that the intrinsic Notch signaling defects that we observe in ciliary mutants might be attributable to disrupted polarized trafficking resulting from ciliary loss. To dissect the molecular mechanisms by which cilia may influence the regulation of Notch signaling, we complemented in vitro culturing of epidermal keratinocytes with our powerful in utero lentiviral delivery method to selectively and efficiently transduce the skin epithelium of embryonic day (E) 9.5 embryos at a stage when it exists as a single-layer of progenitors (Beronja et al., 2010). Using an array of complex genetics, cell biology, and site-directed mutagenesis in developing embryonic epidermis, we demonstrate that Notch-processing enzyme Presenilin-2 targets to the basal body (centrosome), and this localization is required for proper differentiation and optimal activation of Notch signal transduction. We next examine a subset of putative cilia and ciliopathy-related proteins implicated in regulating either Notch signaling or trafficking to primary cilia. Our findings implicate the small GTPase ARF4, which functions in polarized exocytosis (Deretic and Wang, 2012). When ARF4 is absent, cilia are still present, but Presenilins no longer localize to basal bodies and Notch signaling and epidermal differentiation is perturbed.

Results

Notch signaling is spatially associated with ciliogenesis in developing embryonic epidermis

We began by examining Notch activity in detail during embryonic skin development and epidermal differentiation. We used the GFP-transgenic Notch reporter (GFP-TNR) mouse, which has been reported to faithfully recapitulate Notch signaling in the developing nervous system (Gaiano et al., 2000). Confocal microscopy of whole-mount (WM) epidermis showed that GFP-TNR activity was only robust in a subset of epidermal cells within the planes of the first and second suprabasal (spinous) layers of developing E17.5 epidermal tissue (Fig. 1 A). By comparison, Notch reporter activity was considerably lower both within the basal epidermal plane and also in the third and more upper suprabasal spinous layer.

GFP-TNR epifluorescence appeared to faithfully recapitulate epidermal Notch signaling, as judged by immunolabeling for NICD, which displayed strong nuclear localization primarily in the first suprabasal layers (Fig. 1 B, sagittal section). Additionally, expression of the Notch ligand Jagged 1 and the downstream transcriptional activator HES1 was restricted to the first several suprabasal layers of the developing skin epidermis (Fig. 1, C and D). Collectively, these data indicated a spatial activation of Notch signaling within the early embryonic epidermis.

While examining Notch activity in the early differentiating layers of developing skin epidermis, we became intrigued that neither the Notch reporter nor immunolabeling for processed Notch (NICD) and the NICD-RBPj target HES1 was uniform within the spinous layer planes of the epithelium (Fig. 1; Blanpain et al., 2006). To explore this further, we examined the status of primary cilia, which can be visualized using antibodies against either acetylated tubulin or ARL13b. As shown by WM imaging in Fig. 2 A, cilia were readily detected in both basal and spinous layers of E17.5 epidermis. Notably, however, some suprabasal cells did not display a primary cilium (see boxed area in Fig. 2 A; magnified in Fig. 2 B). When examined in
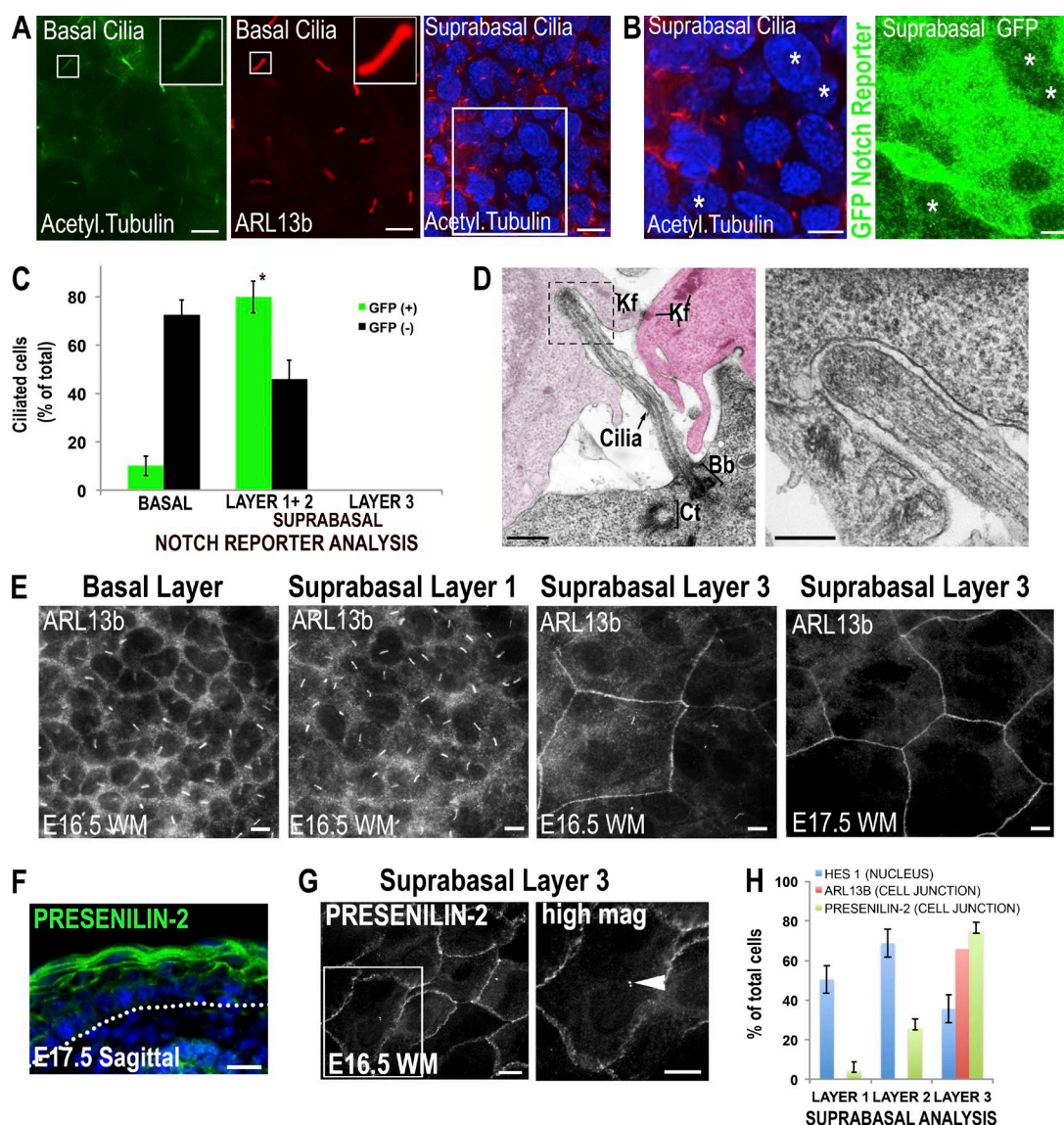
Figure 2. **Notch signaling is associated with ciliogenesis in differentiating embryonic epidermis but is diminished upon localization of ARL13b and Presenilin-2 to cellular junctions.** (A) E17.5 epidermis immunolabeled with an antibody against acetylated tubulin (green) or ARL13b (red) to visualize primary cilia in either basal or suprabasal layers. (B) Image of suprabasal ciliated cells (magnified from boxed region in A), colabeled for the Notch reporter GFP-TNR. Note that in the suprabasal layers, a good correlation exists between GFP-TNR expression and ciliation. In contrast, nonciliated cells within the same suprabasal plane display low GFP-TNR expression (indicated by an asterisk). (C) Quantification of the number of cilia in GFP (+) vs. GFP (−) E17.5 TNR epidermis. Histogram shows percentage of ciliated cells per confocal plane and is an mean of data from three embryos. Error bars are SEM. *, P < 0.05, Student's *t* test. (D) Transmission electron microscopy of E17.5 WT epidermis, showing an example of a primary cilium from one cell appearing to "poke into" an adjacent cell. Suprabasal cells are false-colored pink to highlight their position relative to ciliated cell below. Kf, keratin filaments. Image from boxed panel is magnified at right; note the plasma membrane of one cell juxtaposed with ciliary membrane from neighboring cells. (E) Single confocal planes either basal or suprabasal layers (as indicated) of E16.5–E17.5 WM epidermis immunolabeled with an antibody against ARL13b. Note junctional localization in upper suprabasal layers. (F) Sagittal section of E17.5 epidermis immunolabeled with antibody to Presenilin-2 (green) and DAPI (blue) to mark chromatin. Note junctional localization of Presenilin-2 in the upper suprabasal layers. (G) Single confocal plane of E16.5 WM epidermis immunolabeled with an antibody against Presenilin-2. Boxed region is shown magnified in right panel; arrowhead points to basal body. (H) Quantification of the percentage of cells in the three different suprabasal layers of developing skin that show either nuclear HES1 or junctional Presenilin-2 and ARL13b immunolabeling. Data in histogram were analyzed from E17.5 epidermis; *n* = 2 embryos per condition. Error bars are SEM. Bars: (A–C, E, and G) 15 μm; (D) 0.5 μm; (F) 30 μm.

GFP-TNR embryos, it was readily apparent that those suprabasal cells lacking a visible primary cilium often showed low levels of GFP-TNR activity (Fig. 2 B, cells marked by an asterisk). This became even more apparent in the third and higher suprabasal layers, where cilia were rare. Quantifications indicated that in total, ∼80% of GFP (+) suprabasal cells were ciliated in the first two spinous layers, whereas only 30–40% of GFP (−) cells displayed primary cilia (Fig. 2 C). This differed from the basal layer, where cells were uniformly ciliated with little or no Notch signaling, a feature likely attributed to the largely suprabasal localization of Notch receptors 1–3 in E17.5 epidermis (Blanpain et al., 2006; Williams et al., 2011).

The statistically significant correlation of ciliogenesis with Notch reporter activity suggested that either directly or indirectly, cilia might function in spatially or temporally modulating Notch signaling during the rapid epidermal stratification

that occurs at E15.5 to E17.5. In contrast to Shh, which signals long-range to activate cilia-localized Shh receptors and their downstream effectors (GLI family members; Rohatgi et al., 2007; Kim et al., 2009), Notch ligands are on the surface of juxtaposed cells to signal locally to their Notch-receptor–positive neighbors. Notch ligands are expressed basally (Delta and Jagged 2) as well as suprabasally (Jagged 1; Fig. 1 C; Watt, 2002), offering multiple routes for activating Notch signaling in the spinous cells. To this end, we wondered whether primary cilia might be spatially organized within tissue in such a way that cell-cell signaling, as typified by Notch, might be modulated. A priori, given the stratified nature of the developing epithelia, primary cilia could either poke up in between cells or protrude into a neighboring cell. Electron microscopy of sagittal sections of the ciliary axoneme revealed that the primary cilium of one epidermal cell protrudes into another neighboring cell, thereby juxtaposing the ciliary membrane of one cell with the plasma membrane of its neighbor (Fig. 2 D). By increasing the surface area of cell–cell contact, this spatial positioning of primary cilia within stratified differentiating epidermis could enhance cell–cell signaling for any transmembrane receptors that might exist within the primary cilium in the skin epithelium and whose activating ligands exist within the adjacent cell.

Loss of Notch signaling in upper suprabasal cells is associated with the junctional localization of ARL13b and Presenilin-2

Our studies indicate that Notch signaling is enhanced preferentially in individual suprabasal epidermal cells that are ciliated. Next, we examined the more superficial differentiating cells where TNR-GFP signal, NICD, and HES1 expression waned. Interestingly, although Arl13b beautifully labeled the primary cilia in the basal progenitors and cells within the first two to three layers (Fig. 2, A and E), Arl13b immunolabeling became junctional in the most apical region of cells within more superficial layers (Fig. 2 E and Video 1). Intriguingly, this was reminiscent of the centrosomal protein NINEIN, which was reported to relocalize to the intercellular junctions during epidermal differentiation (Lechler and Fuchs, 2007). Presenilin-2 also localized to both centrosomes/basal bodies and cellular junctions in the epidermis, with enhanced junctional immunostaining in more superficial layers (Fig. 2, F and G; and Video 2). Quantification of the data from Figs. 1 and 2 suggests an inverse correlation between the suprabasal cells in which Presenilin-2 and ARL13b localized to intercellular junctions and HES1, indicative of active Notch signaling (Fig. 2 H). Conversely, HES1 was most readily detected in those epidermal layers where ARL13b and Presenilin-2 localized to cilia and basal bodies, respectively. Collectively, these observations suggest that relocalization of proteins from the cilia or basal bodies (in differentiating cells with high Notch signaling) to cellular junctions (in differentiating cells with low Notch signaling) could contribute to the spatial and temporal activation of Notch signaling observed during epidermal development.

Presenilin-2 localizes to basal bodies through a VxPx C-terminal motif

Genetic ablation studies have previously established a critical role for the two mouse Presenilins in Notch signaling within the skin epidermis (Pan et al., 2004). Presenilin-2 localization can be recapitulated in in vitro studies, where a shift to high (2 mM) calcium prompts intercellular junction formation and terminal

differentiation of cultured primary mouse epidermal keratinocytes (1°MKs). As shown in Fig. 3 A, Presenilin-2 colocalized with γ-tubulin at the centrosome or basal body and, in addition, showed strong labeling at intercellular junctions between keratinocytes. In contrast, lentiviral-mediated shRNA delivery and knockdown (KD) of *Psen2,* but not control (*Scramble*), resulted in a complete loss of Presenilin-2 immunostaining, without loss of cilia per se (Fig. 3 B). Additionally, as judged by Western blot analysis, NICD levels were appreciably reduced in Presenilin-2–deficient (*Psen2*-shRNA KD) keratinocytes (Fig. 3 C). Together, these findings underscored the efficacy of the immunostaining pattern and were in agreement with the prior demonstration of the importance of Presenilins for Notch-signaling in differentiating keratinocytes.

To assess whether basal body localization of Presenilin-2 matters for Notch signaling in the context of epidermal differentiation, we sought to determine how Presenilin-2 localizes to the basal body. In this regard, we were intrigued by the presence of a conserved sequence VRPF within the C-terminal domain of Presenilin-2. Mutations in a similar VxPx motif in Rhodopsin disrupt its localization to the cilia of photoreceptor cells and have been linked to retinitis pigmentosa in humans (Mazelova et al., 2009), and similar mutations in polycystin-2, found in patients with polycystic kidney disease, also result in loss of ciliary localization and function (Ward et al., 2011). Thus, we posited that this sequence in Presenilin-2 might be important for localizing it to basal bodies or cilia during epidermal differentiation.

To test this hypothesis, we designed the *Presenilin* KD and Presenilin-2 rescue strategy illustrated in Fig. 3 D. We generated two lentiviral (LV) expression vectors. One harbored an shRNA that targets both *Psen1* and *Psen2* and a PGK-driven H2B-RFP to control for transduction efficiency; Western blot analysis demonstrated that both Presenilin-1 and Presenilin-2 are effectively depleted using this strategy (Fig. 3 E). The second LV harbored a cDNA expression vector encoding either GFP-Presenilin-2 or GFP-P486A-Presenilin-2, in which the putative VRPF trafficking motif was mutated to VRAF (Figs. 3 D and S1).

Cotransductions into 1°MK were achieved by high titer LV infections confirmed by the presence of both H2B-RFP and GFP-Presenilin. As shown in Fig. 3 F, GFP-Presenilin-2 harboring the wild-type (WT) VRPF motif was detected at both cell junctions and at the cytoplasmic basal body, identified by its colocalization with γ-tubulin. In contrast, P486A-GFP-Presenilin-2, mutated in the putative VxPx trafficking motif, localized to cell junctions, but not to basal bodies, as determined by lack of GFP colocalization with γ-tubulin (representative example shown in Fig. 3 G).

Having confirmed the ability to sever the basal body connection of Presenilins, but not their junctional localization, we then turned to testing the physiological consequences of doing so. For this purpose, we coinjected high-titer ($>10^9$ colony-forming unit) *Psen*1,2 KD and rescue LVs into the amniotic sacs of E9.5 mouse embryos. This noninvasive strategy selectively and efficiently infects and transduces the single-layered embryonic skin epithelium, which stably integrates the LV within 24 h and thereafter propagates it to its progeny (Beronja et al., 2010). Embryos were allowed to develop in utero and then analyzed between E15.5 and birth. Embryos typically showed transduction of >85% head skin and ~60–70% back skin. Because viral DNA stably integrated and embryos grew rapidly, large clonal patches of skin were transduced.
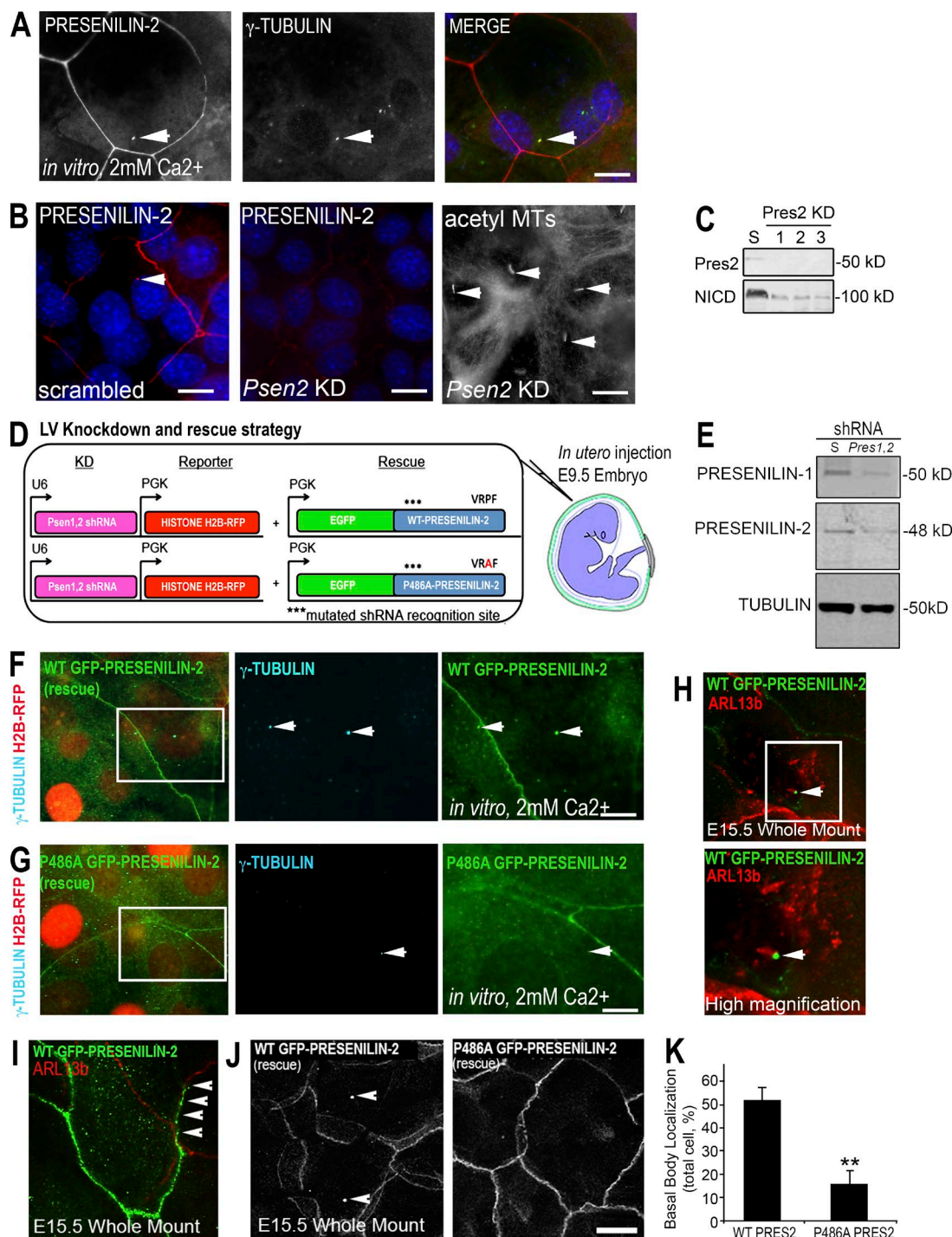
Figure 3. **Presenilin-2 localizes to basal bodies via a VxPx trafficking module in vitro and in vivo.** (A) 1°MKs were induced to differentiate in 2 mM Ca^{2+} and then subjected to IF microscopy with antibodies against Presenilin-2 (red) and γ-tubulin (green). DAPI marks nuclei and arrowheads point to colocalization of Presenilin-2 and γ-tubulin. (B) 1°MKs depleted of Presenilin-2 and immunolabeled for antibodies against Presenilin-2 (to verify KD) or acetylated microtubules (MTs) to visualize cilia (and other stable microtubules within the cell). Arrows point to cilia. (C) Western blot analysis of cell lysates from 1°MKs depleted of Presenilin-2 with one of three different shRNAs and then probed with antibodies against Presenilin-2 and NICD1. Tubulin was used as a loading control (not depicted). (D) Schematic of the LV-mediated expression constructs used for shRNA KD and rescue. High-titer viruses were used for injection into the amniotic sacs of E9.5 embryos as described in the text. (E) Western blots of lysates from keratinocytes transduced with *Psen1,2* shRNA LV and probed with antibodies against Presenilin-1, Presenilin-2, and tubulin (shown as loading control). (F and G) Expression of LV WT GFP-Presenilin-2 or P486A (VxPx mutant) GFP-Presenilin-2 in differentiating cultured keratinocytes, colabeled with γ-tubulin (blue) to visualize basal bodies/centrosomes (arrows). Merged image shows junctional and basal body colocalization of GFP-Presenilin-2 (green) and γ-tubulin (blue). Note that in contrast, the P486A mutant only localized to cell junctions (better visualized in J). Boxed region shown in panels at left are magnified in the two panels at right, and arrows point to basal bodies. (H) Localization of ARL13b (red) and WT GFP-Presenilin-2 (green) in E15.5 epidermis. High-magnification image from boxed region shows example of cilia or basal body localization of GFP-PRESENILIN (arrowhead). (I) ARL13b (red) at nascent WT GFP-Presenilin-2 (+) cell junctions in stratifying E15.5 epidermis. (J) Single confocal plane from E15.5 WM epidermis transduced with *Psen1,2* shRNA and either WT Presenilin-2 GFP or P486A Presenilin-2 GFP, and arrows point to basal body. Bars, 15 µm. (K) Quantification of basal body localization of WT or P486A Presenilin-2; quantification represents data from WM epidermis from at least three different embryos. Error bars are standard deviation. *, P < 0.001, Student's *t* test.

Analysis of E15.5 WM epidermis revealed WT GFP-Presenilin-2 at basal bodies of ARL13b-labeled cilia (Fig. 3 H). In suprabasal cells, WT GFP-Presenilin-2 also showed prominent labeling at cell–cell contacts (Fig. 3, I and J), consistent with the labeling patterns of endogenous protein (Figs. 2 and 3). In contrast, but consistent with our in vitro studies, P486A GFP-Presenilin-2 was only detected at intercellular junctions and not at basal bodies (Fig. 3 J). Quantifications revealed that 50–60% of cells expressing WT GFP-Presenilin-2 showed basal body localization, whereas <20% of cells expressing P486A GFP-Presenilin-2 displayed a basal body-localized GFP signal (Fig. 3 K). These data indicate that the VRPF motif is necessary for localization of PRESENILIN-2 to basal bodies or cilia in both differentiating keratinocytes and developing embryonic epidermis.

The VxPx motif is required to rescue differentiation and Notch signaling defects in Presenilin-deficient epidermis or keratinocytes

To determine whether Presenilin-2 basal body localization is required for efficient activation of Notch signaling in developing epidermis, we evaluated Notch signaling and differentiation markers in *Psen1,2*-depleted epidermis or epidermis cotransduced with WT or P486A GFP-Presenilin-2. shRNA-mediated depletion of both *Presenilins* 1 and 2 (*Psen1,2*) in vivo resulted in a loss of Presenilin immunofluorescence (IF; Fig. 4 A). Additionally, *Psen1,2* KD resulted in a marked reduction in expression of terminal differentiation markers K10 and filaggrin, as well as a loss of NICD nuclear immunolabeling (Fig. 4, B–D).

Psen1,2 KD epidermis expressing WT GFP-tagged Presenilin-2 showed a partial rescue of K10 and filaggrin (Fig. 4, A–C, middle). In contrast, the GFP-tagged Presenilin-2 VRAF mutant P486A showed little or no improvement in rescuing the differentiation defects caused by *Psen1,2* KD (Fig. 4, A–C, right). Similar results were obtained in cultured primary keratinocytes transduced with *Psen1,2* ± WT or mutant GFP-Presenilin-2 (Fig. 4, E and F).

Finally, and in agreement with the results on epidermal differentiation, only the WT GFP-Presenilin-2, and not the P486A GFP-Presenilin-2 mutant, showed rescue of suprabasal nuclear NICD. Thus, as shown by the quantifications in Fig. 4 G, when *Psen1,2* were depleted, <10% of H2B-RFP (+) nuclei colocalized with nuclear NICD signal, consistent with the known requirement of both Presenilins in regulating NICD processing in the developing epidermis (Pan et al., 2004). Upon coexpression with WT Presenilin-2 GFP, 25% of H2B-RFP (+) nuclei were NICD immunolabeled, whereas very little improvement in NICD was seen with the P486A presenelin-2 mutant (Fig. 4 G). These data suggest that the VxPx trafficking motif of Presenilin is required for optimal Notch signaling and epidermal differentiation.

A subset of cilia/ciliopathy-related proteins are required for K10 expression and Notch reporter activity in differentiating 1°MKs

Polarized exocytosis has emerged as a primary mechanism for delivering proteins to the primary cilia (Jin et al., 2010). Our observations suggest that a conserved VxPx trafficking motif targets Presenilins to basal bodies or cilia and that this subcellular localization is required for optimal Notch signaling and epidermal differentiation during development.

To determine if known ciliary trafficking mechanisms contribute to Presenilin localization and activation of Notch signaling, we examined a panel of candidate cilia/ciliopathy-related proteins and used shRNA-mediated KD to ascertain their contribution to differentiation and Notch signal transduction in 1°MKs. Upon a shift to high Ca^{+2}, cells were analyzed for keratinocyte differentiation (K10) or GFP (Notch reporter activity). The data were quantified as shown in Fig. 5 (A and B). As expected from our previous study (Ezratty et al., 2011), KD of either *Ift74* or *Ift88* significantly diminished not only K10, but also Notch reporter expression in most transduced cells. *Pin1* KD also showed a marked inhibition of both K10 and Notch reporter expression. We included *Pin1*, encoding a prolyl isomerase, because it had surfaced in a proteomic analysis of primary cilia (Ishikawa et al., 2012) and also was previously shown to stabilize and/or enhance Notch activity (Rustighi et al., 2009; Baik et al., 2015). Our focus was on a subset of ARL/ARF family small GTPases (Zhang et al., 2013) that, when knocked down, showed a marked reduction in overall levels of K10 and Notch reporter expression (Fig. 5, A and B). These proteins had not been previously implicated in epidermal differentiation or Notch signaling.

The small GTPase ARF4 is required for epidermal differentiation and Notch signaling in vitro and in vivo

We focused on ARF4, a small GTPase that recognizes VxPx trafficking motifs (Mazelova et al., 2009). We used BBS2 as a control, because the BBSome has also been implicated in trafficking to the basal body, yet *Bbs2* shRNAs showed little or no effect on K10 or GFP-TNR expression (Fig. 5, A and B; IF examples in Fig. 5, C and D). As shown in Fig. S2, both *Arf4* and *Bbs2* shRNAs knocked down their respective proteins as judged by IF and/or immunoblot analyses. These data suggest that the defects in K10 and GFP-TNR expression could be attributable to a specific role for ARF4 trafficking in regulating aspects of Notch signaling rather than a general defect associated with disruption of trafficking via other basal body–associated trafficking modules (such as the BBSome).

To ascertain the effects of ARF4 on epidermal differentiation in vivo, we cloned a second, equally strong shRNA *Arf4-2* and scrambled control shRNA into lentiviral H2B-RFP expression vectors and injected them into amniotic sacs of living E9.5 mouse embryos in utero. Although the data shown are for *Arf4-2*, similar results were obtained with *Arf4-3*. Consistent with defective Notch signaling, clones of *ARF4-2* shRNA epidermis showed reduced K10 (Fig. 5 E). Importantly, K10 was still expressed in adjacent uninfected skin patches, suggesting that the defects in epidermal differentiation were cell-autonomous and not caused by general skin perturbations. Epidermis depleted of ARF4 also showed marked defects in the expression of key terminal differentiation markers filaggrin and loricrin (Fig. 5, F and G), when compared with either scrambled control epidermis (Fig. 5, F and G) or nontransduced littermate controls (not depicted). These data suggest that ARF4 is required for efficient epidermal differentiation during development.

ARF4-deficient epidermal keratinocytes and embryos generate cilia but show signs of ciliary dysfunction

ARF4 and BBS2 are both known to be required for trafficking of ciliary localized proteins and ciliary signaling, but not for ciliogenesis (Follit et al., 2014). Consistent with this notion,
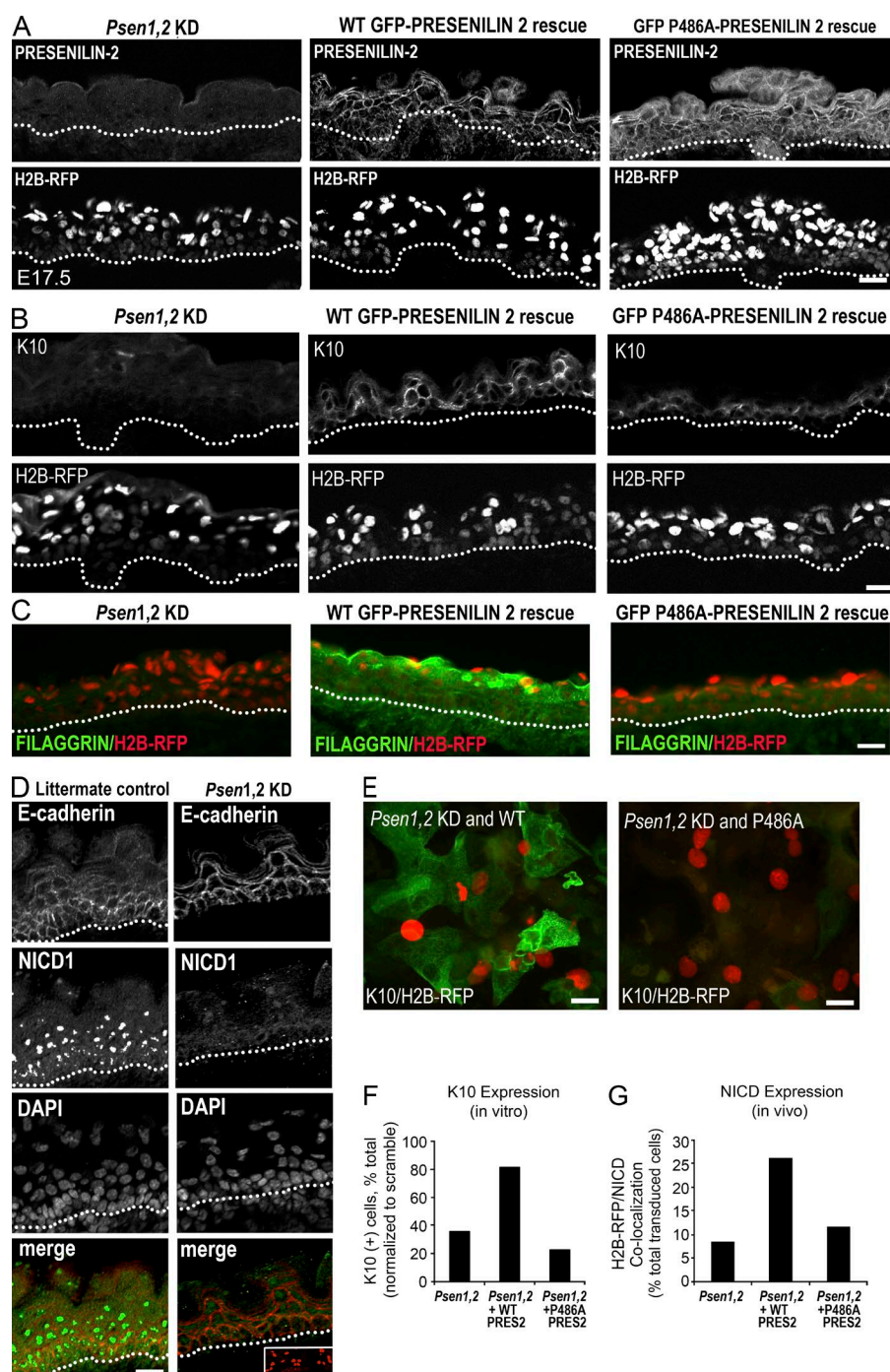
Figure 4. **Presenilin-2 localization at basal bodies is required to efficiently rescue differentiation and Notch-signaling defects in embryos and cultured keratinocytes depleted of Presenilin-1 and Presenilin-2.** (A) E17.5 epidermis was transduced at E9.5 with *Psen*1-2 shRNA (H2B-RFP) alone or with WT GFP-Presenilin-2 or GFP-P486A Presenilin-2, and then subjected to IF microscopy with an antibody against Presenilin-2. (B and C) Images of *Psen*1-2 KD versus a rescue experiment showing transduction with WT or P486A GFP-Presenilin-2 (as shown in A), immunolabeled with antibody against K10 or filaggrin. H2B-RFP marks regions transduced with the *Psen*1,2 shRNA LV. (D) Control or *Psen*1-2 KD epidermis immunolabeled with antibodies against E-cadherin or NICD 1 or counterstained with DAPI. Merged image shows NICD/ECAD overlay. (E) Images of differentiating keratinocytes cultured in 2 mM Ca^{2+} and immunolabeled with antibody against K10 (green). H2B-RFP (red nuclei) marks regions transduced with *Psen*1-2 shRNA and either WT GFP-Presenilin-2 or P486A GFP-Presenilin-2. (F) Quantification of K10 expression in differentiating keratinocytes transduced with *Psen*1-2 shRNA alone or rescued with WT or P486A Presenilin-2 GFP. Data in histogram are normalized to scrambled control and represent data from two independent experiments. (G) Quantification of NICD (Notch intracellular domain) and H2B-RFP co-localization in E17.5 epidermis from embryos transduced with *Psen*1,2 shRNA alone or with either WT or P486A Presenilin-2 GFP. The percentage of total nuclear area in suprabasal cells expressing H2B-RFP was measured and compared with the percentage of total nuclear area NICD expression (see Materials and methods). Bars: (A–D) 30 µm; (E) 15 µm.

differentiating 1°MKs that had been depleted of either ARF4 or BBS2 still generated cilia (Fig. 6 A, representative cilia are shown at higher magnification on right). Cilia were also present when ARF4 was depleted in vivo, as illustrated best by WM IF confocal microscopy (Fig. 6 B, right panel is a magnified view of boxed region from the left panel). Collectively, these findings uncouple the epidermal differentiation defects from ciliogenesis.

Interestingly, most *Arf4-2* (or *Arf4-3*), but not *scrambled*, transduced embryos displayed polydactyly of both hind and forelimbs (Fig. 6 C). This feature is a classical sign of overactive SHH signaling by loss of GLI3, a transcription factor

downstream of SHH that typically functions as a repressor. Notably, however, polydactyly is also seen in double loss-of-function mutations for both *Shh* and *Gli3* (Litingtung et al., 2002), i.e., analogous to what would be expected in ciliogenesis mutants. Based upon these data, ciliary function and epidermal differentiation appeared to be compromised by loss of ARF4 in the skin epithelium, even though the primary cilia were still intact. These data suggest that the differentiation defects we observe in the ARF4-depleted epidermis are not caused by ciliogenesis defects per se, although trafficking within cilia could still be perturbed as suggested by the polydactyly phenotype of *Arf4* KD embryos.
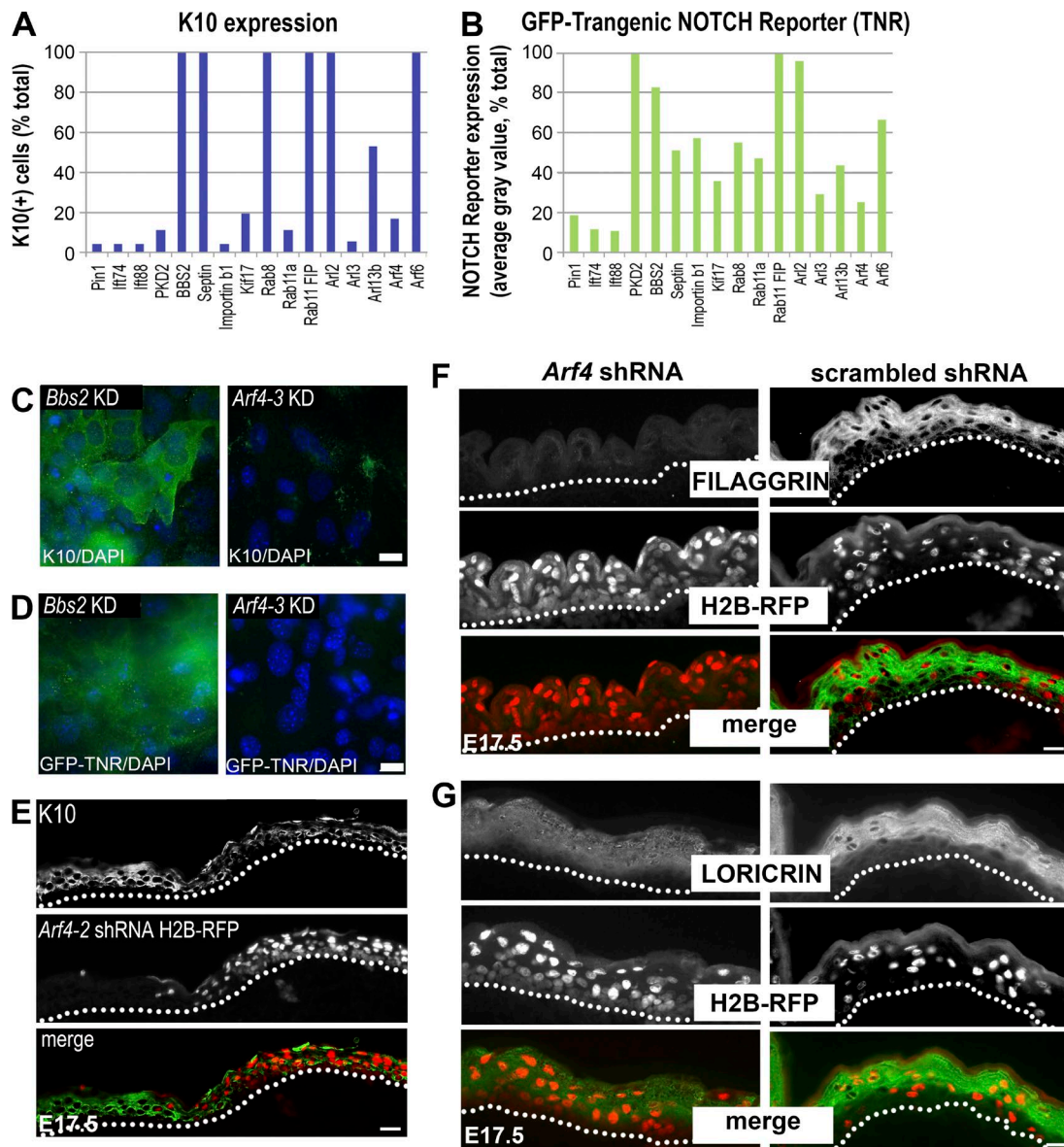
Figure 5. **The small GTPase ARF4 is required for K10 and Notch reporter expression and epidermal differentiation.** (A and B) Quantification of K10 or GFP-TNR (Notch reporter) expression in 1°MKs transduced with pooled shRNAs against the indicated ciliary and trafficking proteins. Histograms represent data from two individual experiments where pooled shRNAs were transduced to cultured keratinocytes before differentiation, and the percentage of K10 (+) or GFP (+) cells was quantified after 48-h Ca²⁺ addition to induce differentiation. (C and D) Images of differentiating 1°MKs transduced with *Arf4* or *Bbs2* shRNAs and then immunolabeled with antibodies against K10 or tested for Notch reporter activity. DAPI used to visualize nuclei. (E) Example of *Arf4-2* shRNA transduced tissue adjacent to nontransduced epidermis. IF is for K10 (green) to mark epidermal differentiation and H2B-RFP (red) to mark transduced cells. (F and G) Example of *Arf4-2* or *scrambled* control shRNA transduced tissue immunolabeled for antibodies against FILAGGRIN or LORICRIN (green). H2B-RFP (red) marks transduced cells. Bars, 30 µm.

ARF4-dependent trafficking of Notch components is required for Notch signaling in vitro and in vivo

ARF4 has been implicated in Golgi to basal body trafficking (Deretic and Wang, 2012), and our mutagenesis studies suggest that localization of Presenilin-2 to basal bodies is important for robust Notch signal transduction and epidermal differentiation. In contrast to a *Scrambled* control shRNA, where Presenilin-2 was localized to basal bodies, *Arf4* KD led to intracellular accumulation of Presenilin-2 (Fig. 7 A). Quantification of Presenilin-2 localization to basal bodies revealed that, as previously shown, 50% of cells had Presenilin-2 localized at basal bodies, but only 10% of *Arf4* KD cells showed this localization (Fig. 7 B).

Consistent with a defect in polarized trafficking, immunolocalization also revealed what appeared to be an accumulation of Notch receptor in a perinuclear compartment that colocalized with GM130, a marker for the Golgi apparatus (Fig. 7 C). Quantifications revealed significantly reduced levels of Notch 2 and Golgi IF in control as compared with *Arf4* KD keratinocytes. These data suggest that ARF4 may regulate trafficking of Notch components, because aberrant accumulation of Presenilin-2 and Notch 2 were observed upon *Arf4* depletion during keratinocyte differentiation. In vivo, Notch 2 also accumulated in what appeared to be a perinuclear localization in suprabasal, but not basal, cells of *Arf4* KD epidermis (Fig. 7 E). Expression of the downstream NICD/Rbpj target gene *Hes1* was also
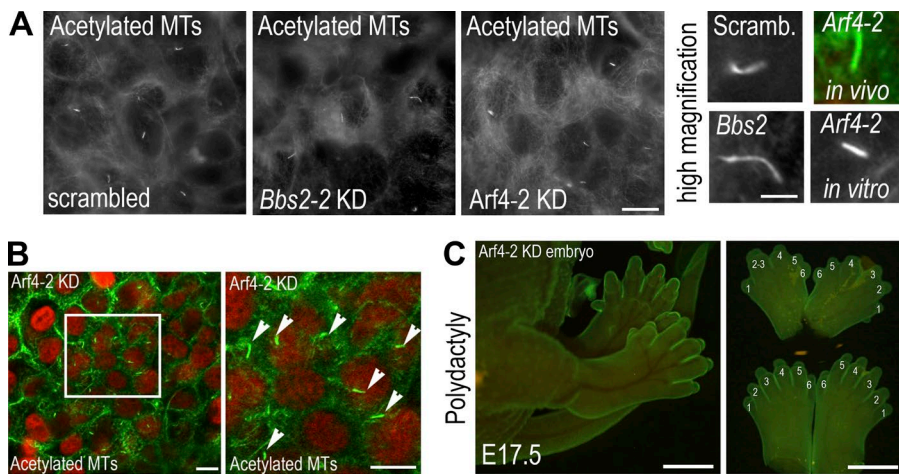
Figure 6. **ARF4 is not required for ciliogenesis in vivo or in vitro, but its loss results in polydactyly.** (A) Images of differentiating keratinocytes transduced with *scrambled* control, *Arf4*, or *Bbs2* shRNAs and then immunolabeled with antibodies against acetylated tubulin to visualize stable microtubules, including primary cilia. See magnified examples in the panels at the right, showing that cilia still form upon depletion of either of these proteins. Bars: 15 μm; (high-magnification cilia) 1 μm. (B) Single confocal plane of E15.5 WM epidermis immunolabeled with an antibody to acetylated tubulin (green). H2B-RFP (red) marks transduced cells. Boxed image at left is shown magnified at right. Arrows point to primary cilia. Bars, 15 μm. (C) Image of E17.5 embryo transduced with *Arf4-2* shRNA, showing examples of polydactyly, observed in 75% of ARF4 KD embryos examined. Bars, 1 mm.

significantly reduced in the absence of ARF4 function (Fig. 7 F). Collectively, these observations suggest that ARF4-dependent trafficking of Notch components contributes to proper activation of Notch signaling and is required for robust epidermal differentiation during development.

Discussion

In the present study, we extended the curious links among Notch signaling, cilia, and epidermal differentiation that we and others have observed in mice (Croyle et al., 2011; Ezratty et al., 2011). Although ciliogenesis is downstream of Notch signaling in most tissues, in the developing epidermis, cilia are present as early as E11.5, when skin is a single-layered epithelium, and before, when either Notch signaling or Shh signaling acts in epidermal or HF morphogenesis, respectively (Oro and Higgins, 2003; Ezratty et al., 2011; Williams et al., 2011). Our findings that Notch 2, Notch 3, and Presenilin-2 immunolocalize to primary cilia and/or basal bodies and that ciliogenesis is temporally and spatially associated with Notch reporter activity and differentiation during embryonic skin development have provided a framework with which to probe deeper into the context-specific role of primary cilia and its potential regulation of Notch signal transduction.

Trafficking of Notch components to and from primary cilia: a role for ARF4

Our study revealed a role for the small GTPase ARF4 in epidermal differentiation and Notch signaling both in cultured keratinocytes and in developing embryonic skin. Consistent with other studies, we found that ARF4 is not required for ciliogenesis in keratinocytes (Follit et al., 2014). Rather, it appears to participate in trafficking Notch components from the Golgi to basal bodies or primary cilia. *Arf4* knockout mice die at midgestation (E9.5–10.5), shortly before node formation, and display trafficking defects in nonciliated endoderm but normal left–right patterning, a feature dependent on ciliogenesis (Follit et al., 2014). Although the early embryonic lethality of these mice precluded an analysis of skin differentiation and development, it is interesting that ARF4 has been implicated in megalin and fibrocystin trafficking, as both of these proteins undergo intracellular proteolysis, regulated by either γ-secretase (Presenilin) or γ-secretase–like enzymes (Biemesderfer, 2006; Kaimori et al., 2007). Given our findings, we hypothesize that ARF4 may

play a general role in regulating the trafficking of membrane receptors that are destined for regulated intracellular proteolysis after their activation at specific subcellular structures. Such a function would be independent of whether the trafficking occurs at cilia or at some other subcellular structure. According to this paradigm, in the context of skin differentiation, the traffic happens to occur at the basal body or primary cilia, where ARF4 would function in localizing γ-secretase and processing Notch receptors. Although more studies will be needed to corroborate these facets, the model serves to conceptualize the cell type–specific differences in ciliary roles that go beyond Shh signaling and may be relevant for understanding the etiology of ciliopathies that cannot be explained solely via loss of Shh signaling.

Is subcellular proteolysis spatially and temporally regulated at primary cilia?

It is intriguing to speculate that basal bodies/primary cilia might be compartmentalized subcellular domains where regulated intracellular proteolysis occurs in a temporally regulated manner during development. Our observations of Notch reporter activity in developing epidermis suggest that such regulation might occur, and primary cilia are poised to spatially and temporally influence these aspects of Notch signaling.

The proteasome has been localized near centrosomes (Fabunmi et al., 2000), and disruption of basal body proteins, such Bardet–Biedl complex proteins BBS1 and BBS4, compromise proteasomal function that impinges on Wnt signaling (Gerdes et al., 2007). Moreover, such proteins were recently shown to regulate Notch signaling via endosomal trafficking of the Notch receptor in zebrafish (Leitch et al., 2014). This latter study found that loss of BBS1 or BBS4 resulted in increased Notch reporter activity, accompanied by decreased localization of Notch receptor at both primary cilia and the plasma membrane. Consistent with this view, BBS2 loss consistently showed sustained or elevated Notch reporter activity and K10 expression in our studies, whereas depletion of other ciliary or cilia-related proteins consistently suppressed Notch signaling and K10-mediated differentiation in cultured keratinocytes. We did not carefully analyze endosomal trafficking of Notch receptor upon depletion of BBS2, but our results are consistent with the zebrafish studies showing increased Notch activity. Collectively, these data suggest that basal body proteins may have different regulatory functions than proteins found within, or that have access to, the ciliary compartment.
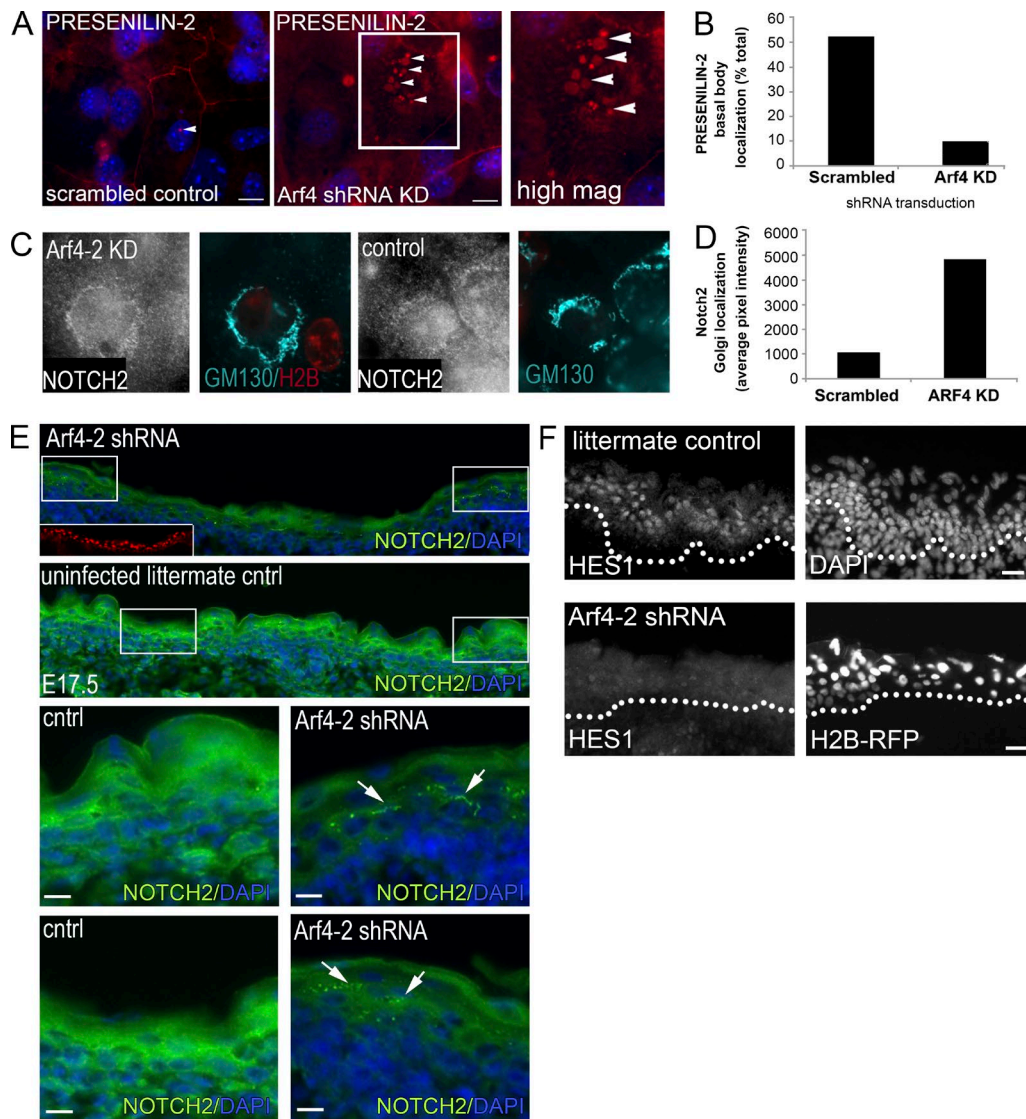
Figure 7. **Depletion of ARF4 results in intracellular accumulation of Notch signaling components in vitro and in vivo and reduced HES1 expression in developing epidermis.** (A) Differentiating cultured keratinocytes infected with LV harboring *Arf4-2* or *scrambled* control shRNA and then immunolabeled for Presenilin-2 (red). DAPI marks nuclei. Arrowheads point to perinuclear vesicular accumulation of presenilin-2 upon depletion of *Arf4*. (B) Quantification of Presenilin-2 basal body localization in *Arf4* KD keratinocytes. Data in histogram are from two independent experiments in which 100–200 cells were analyzed per condition. (C) Differentiating cultured keratinocytes transduced with *Arf4* shRNA and immunolabeled for Notch 2 (gray) and GM130 (cyan) to visualize Golgi. H2B-RFP marks transduced cells (red) versus nontransduced control cells. (D) Quantification of Notch 2-Golgi fluorescence in *Arf4* versus *scrambled* control shRNA-expressing keratinocytes. Data in histogram are from two independent experiments in which 100–200 cells were analyzed per condition. (E) Notch 2 (green) expression in *Arf4-2* shRNA (inset, H2B-RFP nuclei) transduced tissue versus uninfected littermate control. DAPI marks nuclei. Boxed regions are magnified in the images at right. Arrows point to perinuclear accumulation of Notch. (F) Expression of HES1, a downstream Notch target gene, is no longer seen in the suprabasal layers of epidermis that has been depleted of the small GTPase ARF4. Bars: (A–C) 15 µm; (E and F) 30 µm.

Presenilins have been localized to multiple subcellular compartments, mainly the Golgi and endoplasmic reticulum, but to our knowledge, this is the first study to implicate that localization of a Presenilin to basal bodies may have functional consequences in regulating Notch signaling and epidermal differentiation. During mouse preimplantation development, Presenilins redistribute to centrosomes when the proteasome is inhibited (Jeong et al., 2000), and Förster resonance energy transfer studies of APP and Presenilin-1 suggest close interaction at the centrosome in human neuroglioma cells (Nizzari et al., 2007). Additionally, two different proteomic studies of isolated primary cilia detected Presenilins, Notch receptor, and the Notch regulator PIN1 (Ishikawa et al., 2012; Narita et al.,

2012), suggesting that Notch components may be generally present in the cilia/ciliary membrane in at least two different cell types besides keratinocytes. The data further strengthen the notion that Notch components may, in some contexts, be bona fide components of the ciliary proteome.

Our studies manipulating the VxPx trafficking motif of Presenilin-2 lend further support to this notion. The ability of WT, but not P486A mutant, Presenilin-2 to rescue Notch-signaling defects in cells and embryos depleted of both Presenilin-1 and Presenilin-2 underscores the importance of this sequence in targeting to the basal body in the context of epidermal differentiation. One caveat of our studies is that although Presenilin-1 has been detected at cilia in the aforementioned

proteomic studies, we have only been able to detect Presenilin-2 at centrosomes or primary cilia using antibodies or GFP-tagged constructs (unpublished data). This VxPx trafficking motif may alternatively regulate other aspects of the structure or function of Presenilin-2 in addition to its subcellular localization, and it will be important to determine whether this motif is a bona fide ciliary targeting sequence or whether this mutation regulates other aspect of Presenilin biology and Notch signal transduction.

Exo- and endocytosis at primary cilia: implications for the context specific regulation of Notch signaling

Our data support a model where ARF4-dependent exocytosis is required for localization of Presenilin-2 to basal bodies or primary cilia, where γ-secretase has roles in modulating Notch signal transduction, either directly or indirectly. There are likely other levels of regulation of Notch signaling that involve either basal body or primary cilia-dependent mechanisms. One intriguing possibility is that endocytosis of components at the cilia may regulate various aspects of Notch signaling during skin development. The ciliary pocket has been implicated as a "hot spot" for endocytosis (Molla-Herman et al., 2010), and either Notch receptors or perhaps Notch ligands, both of which require endocytosis for proper signaling function, could be selectively or preferentially internalized in this specialized compartment of the plasma membrane.

Another intriguing potential mechanism for Notch regulation at primary cilia involves the newly described release of exosomes from the primary cilia. In *Chlamydomonas reinhardtii*, the cilium has been shown to additionally function as a secretory organelle via release of protease containing ciliary ectosomes (Wood et al., 2013). These lytic-enzyme containing extracellular membrane vesicles function to liberate daughter cells after mitosis. Because Notch receptors undergo a multiplicity of cleavage events, both extra- and intracellularly, it is intriguing to speculate that ciliary-mediated release of a bioactive factor could regulate signal transduction and cell–cell communication. It is currently unknown whether primary cilia in tissue cells, such as those of the stratified skin epithelia, can signal to adjacent cells. Our studies documenting perturbed Notch signal transduction in the absence of cilia and our observations of cilia poking into adjacent cells suggest that primary cilia may regulate cell–cell communication during development and unveil yet another fascinating potential function of the primary cilia that merits additional study.

Materials and methods

Generation of mice

CD-1 mice obtained from The Jackson Laboratory were used for in utero lentiviral injections. TNR mice (Mizutani et al., 2007) were obtained from The Jackson Laboratory and outbred to a CD1 background, where they were maintained as homozygotes.

Cell culture and in vitro lentiviral infection

Primary keratinocytes were isolated from WT CD-1 or TNR mice and cultured using previously described methods (Nowak and Fuchs, 2009). HEK293T cells were obtained from Takara Bio Inc. and used for lentiviral production as previously described. For lentiviral infections, keratinocytes were plated at 100,000 cells per six wells and incubated with lentivirus in the presence of 100 µl polybrene. 24–48 h after viral

infection, cells were selected with 1–2 mg/ml puromycin. 96 h postinfection, keratinocytes were grown to confluency on fibronectin-coated coverslips and shifted to 2 mM Ca²⁺ growth media as previously described (Ezratty et al., 2011). Coverslips were fixed in either −20 Methanol (to visualize the microtubule cytoskeleton) or 4% PFA before processing for IF. Paraformaldehyde-fixed samples were permeabilized for 5 min in 0.5% Triton X-100. All antibodies were diluted in 10% normal goat serum in PBS.

shRNA and DNA constructs and in utero lentiviral injections

In utero injection of E9.5 embryos and production of high-titer lentivirus were performed as previously described and are extensively detailed elsewhere (Beronja et al., 2010). Lentiviral shRNAs were provided by the Broad Institute's Mission TRC-1 Library (Sigma-Aldrich) and for some experiments were cloned from the library vector into a modified pLKO backbone containing H2B-RFP. For the KD panel shown in Fig. 5, five different shRNAs to the proteins indicated from the TRC-1 library were pooled and used to generate lentiviral supernatant for KD. For experiments where individual shRNA were used, the following target sequences were used: Arf4-2, 5′-GCTGTCAAATGA ACTTTCAAA-3′; Arf4-3, 5′-CCACTTGTGCTACACAAGGAA-3′.

For *Psen*1,2 shRNA-mediated targeting both *Psen1* and *Psen2*, the following conserved target sequence was used: 5′-CCTCCCCAT CTCCATCACCTT-3′. The following forward and reverse oligos were synthesized (Operon): 5′-CCGGCCTCCCCATCTCCATCA CCTTCTCGAGAAGGTGATGGAGATGGGGAGGTTTTTG-3′; 5′-AATTCAAAAACCTCCCCATCTCCATCACCTTCTCGAGAAG GTGATGGAGATGGGGAGG-3′.

Oligos were annealed and cloned into pLKO.1-H2B-RFP using previously described methodology (Williams et al., 2011). Full-length mouse cDNA for Presenilin-2 was obtained from OriGene and directionally cloned into pEGFP-N1 (Takara Bio Inc.) via EcoRI and Xba sites. To generate the WT Presenilin-2 GFP lentiviral construct, H2B-RFP was excised from and Presenilin-2 GFP was ligated into pLKO.1 using previously described methodology (Beronja et al., 2010). This plasmid was used as the backbone to generate the P486 Presenilin-2 GFP construct, and the gene mutation was generated using Quick Change II Site-directed Mutagenesis kit (Agilent Technologies) according to the manufacturers protocol. Positive clones were identified and verified via restriction digest of a region predicted to be unique in the mutated clone. For *Psen1,2* KD and presenlin-2 rescue experiments in vitro or in vivo, *Psen*1,2 H2B-RFP pLKO.1 and/or WT Presenilin-2 GFP or P486 Presenilin-2 GFP high-titer LV particles were generated and coinjected in CD-1 WT E9.5 embryos (see schematic in Fig. 3 C).

Embryo preparation and IF

For WM immunofluorescence, embryos were fixed in 4% formaldehyde in PBS for 1 h at room temperature and washed extensively in PBS. Backskins were dissected and then permeabilized for 10 min in 0.3% Triton X-100/PBS and blocked in Gelatin Block (2.5% fish gelatin, 2.5% normal donkey serum, 2.5% normal goat serum, 0.5% BSA, 0.1% Triton X-100, and 1× PBS) containing MOM reagent (Vector Laboratories) for 1 h at room temperature. All primary antibodies were used at 1:200 dilution and incubated overnight at 4°C. Primary antibodies were removed by extensive washing in 0.3% Triton X-100/PBS, followed by 1-h room temperature incubation with secondary antibodies.

For IF on sagittal sections, embryos were embedded and frozen in OCT, cryosectioned (10–12 µm), and fixed 10 min in 4% formaldehyde in PBS. Sections were blocked 1 h in 2.5% fish gelatin, 2.5% normal donkey serum, 2.5% normal goat serum, 0.5% BSA, 0.1% Triton X-100, and 1× PBS. The following primary antibodies were incubated for either 2 h at room temperature or overnight at 4°C at the following

dilutions: mα acetylated tubulin (1:200; Sigma-Aldrich), E-cadherin (1:200; Fuchs laboratory), α-tubulin (1:200; EMD Millipore), rbαK14 (1:400; Fuchs laboratory), rtα Nidogen (1:2,000; Invitrogen), rbα K10 (1:500; Covance), Rb α involucrin (1:1,000; Covance), Rb αfilaggrin (1:1,000; Covance), Rb αHes1 (1:200; Fuchs laboratory), chicken αGFP (1:5,000; Abcam), Rb αGFP (1:5,000; Invitrogen), Rb monoclonal antibody α Notch 1 (4147, 1:200; Cell Signaling Technology) Rbα hamster monoclonal antibody α Notch 2 (1:400; BioLegend), Rb α Notch 3/NICD3 (ab23426, 1:400; Abcam), rbα Presenilin-2 (1:200; Abcam), rbαJagged1 (ab7771, 1:200), rbαPin1 (ab76309, 1:200; Abcam), rbαBBS2 (ab86158, 1:200; Abcam), Rbα GM130 (D1E11, 1:400; Cell Signaling Technology), and Rbα Arf4 (1:200; Abcam). Secondary antibodies conjugated to Alexa Fluor 488 (Molecular Probes), Cy3, RRX, or Cy5 (The Jackson Laboratory) were diluted 1:200–1:500 in gelatin block and incubated 1 h at room temperature. Tissue was extensively washed in PBS before mounting with Pro-Long Gold containing DAPI (Invitrogen).

Western blotting

Cultured keratinocytes lysed in RIPA buffer containing a cocktail of protease inhibitors (Roche). Gel electrophoresis, Western blotting, and infrared imaging were performed as previously described (Ezratty et al., 2011). Primary antibodies used were rat anti–α-tubulin (1:5,000; EMD Millipore), hamster mAb α Notch 3 (1:500; BioLegend), Rb α Notch 3/NICD3 (1:500; ab23426; Abcam), rbα Presenilin-2 (1:10,000; Abcam) mα Presenilin-1. (1:5,000; Abcam) Rbα Arf4 (1:200; Abcam), and rbαBBS2 (1:200; ab86158; Abcam). Secondary antibodies were conjugated to IRDye680 or IRDye800CW (LI-COR Biosciences and Rockland) and were used at 1:15,000.

Confocal microscopy and imaging

Confocal images were acquired with a Zeiss LSM510 laser-scanning microscope (ZEISS) through a 63× oil objective. (N.A. 1.4) For WM imaging, Z-stacks of 20–40 planes (0.25 µm) were captured, but only representative single Z-planes are presented. Images were recorded at either 512 × 512 or 1,024 × 1,024 square pixels. For wide-field epifluorescence, images were acquired using an Axioplan 2 (ZEISS) 20×/0.8 air or 63×/1.4 oil Plan-Apochromat objectives equipped with the following Chroma filter sets: 49003 ET YFP (YFP), 49008 ET TR C94094 (mRFP1), 49004 ET dsR C94093 (Cy3, DyLight549), 41008 Cy5 (Cy5), and 41001 FITC (Alexa Fluor 488/GFP).

Quantification and statistical analysis

For quantification of HES1 (nuclear) versus ARL13b/Presenilin-2 (junctional) staining, the number of nuclei in either sagittal or single confocal planes of E17.5 epidermis was determined by thresholding the DAPI or HES1 image in ImageJ and using the measure function to count the number of nuclei, and then cell junction staining was manually determined on the basis of its appearance in various epidermal layers. Suprabasal layers 1–3 were manually determined and ImageJ was used to select layers for analysis as described. For quantification of ciliogenesis, K10 or Notch reporter expression during epidermal development or in cultured keratinocytes, the number of nuclei were determined in single confocal planes by thresholding the image (either DAPI or H2B-RFP [+] nuclei) in ImageJ and using the Measure function to count the number of objects. The number of cilia/K10[+]/GFP^{+} cells were then manually counted in either basal or suprabasal single confocal planes. For quantification of Presenilin-2 basal body localization, the number of nuclei was determined using the measure function in ImageJ, and then the number of basal bodies with a GFP-Presenilin-2 signal was manually determined in single confocal planes of suprabasal cells. For quantification of H2B-RFP/NICD colocalization in Presenilin rescue experiments, the

colocalization function in Metamorph was applied to thresholded images and the total pixel area of colocalization was determined and expressed as a percentage of the total nuclear area. Unless otherwise noted, all error bars represent SEM, and an unpaired two-tailed Student's t test was performed on datasets collected from multiple independent experiments to determine statistical significance where indicated.

Online supplemental material

Fig. S1 shows relative levels of expression of WT GFP-Presenilin-2 versus P486-GFP-Presenilin-2 in cultured keratinocytes. Fig. S2 shows immunofluorescence and a Western blot of BBS2 or ARF4 in keratinocytes transduced with indicated shRNAs. Video 1 shows a confocal stack of E16.5 epidermis stained with an antibody against Arl13b. Video 2 shows a confocal stack of E16.5 epidermis stained with antibodies against acetylated tubulin and Presenilin-2. DAPI labels nuclei. Online supplemental material is available at http://www.jcb.org/cgi/content/full/jcb.201508082/DC1.

References

Badano, J.L., N. Mitsuma, P.L. Beales, and N. Katsanis. 2006. The ciliopathies: an emerging class of human genetic disorders. *Annu. Rev. Genomics Hum. Genet.* 7:125–148. http://dx.doi.org/10.1146/annurev.genom.7.080505.115610

Baik, S.H., M. Fane, J.H. Park, Y.L. Cheng, D. Yang-Wei Fann, U.J. Yun, Y. Choi, J.S. Park, B.H. Chai, J.S. Park, et al. 2015. Pin1 promotes neuronal death in stroke by stabilizing Notch intracellular domain. *Ann. Neurol.* 77:504–516. http://dx.doi.org/10.1002/ana.24347

Berbari, N.F., A.K. O'Connor, C.J. Haycraft, and B.K. Yoder. 2009. The primary cilium as a complex signaling center. *Curr. Biol.* 19:R526–R535. http://dx.doi.org/10.1016/j.cub.2009.05.025

Beronja, S., G. Livshits, S. Williams, and E. Fuchs. 2010. Rapid functional dissection of genetic networks via tissue-specific transduction and RNAi in mouse embryos. *Nat. Med.* 16:821–827. http://dx.doi.org/10.1038/nm.2167

Biemesderfer, D. 2006. Regulated intramembrane proteolysis of megalin: linking urinary protein and gene regulation in proximal tubule? *Kidney Int.* 69:1717–1721. http://dx.doi.org/10.1038/sj.ki.5000298

Blanpain, C., W.E. Lowry, H.A. Pasolli, and E. Fuchs. 2006. Canonical notch signaling functions as a commitment switch in the epidermal lineage. *Genes Dev.* 20:3022–3035. http://dx.doi.org/10.1101/gad.1477606

Croyle, M.J., J.M. Lehman, A.K. O'Connor, S.Y. Wong, E.B. Malarkey, D. Iribarne, W.E. Dowdle, T.R. Schoeb, Z.M. Verney, M. Athar, et al. 2011. Role of epidermal primary cilia in the homeostasis of skin and hair follicles. *Development.* 138:1675–1685. http://dx.doi.org/10.1242/dev.060210

Deretic, D., and J. Wang. 2012. Molecular assemblies that control rhodopsin transport to the cilia. *Vision Res.* 75:5–10. http://dx.doi.org/10.1016/j.visres.2012.07.015

Ezratty, E.J., N. Stokes, S. Chai, A.S. Shah, S.E. Williams, and E. Fuchs. 2011. A role for the primary cilium in Notch signaling and epidermal differentiation during skin development. *Cell.* 145:1129–1141. http://dx.doi.org/10.1016/j.cell.2011.05.030

Fabunmi, R.P., W.C. Wigley, P.J. Thomas, and G.N. DeMartino. 2000. Activity and regulation of the centrosome-associated proteasome. *J. Biol. Chem.* 275:409–413. http://dx.doi.org/10.1074/jbc.275.1.409

Follit, J.A., J.T. San Agustin, J.A. Jonassen, T. Huang, J.A. Rivera-Perez, K.D. Tremblay, and G.J. Pazour. 2014. Arf4 is required for Mammalian development but dispensable for ciliary assembly. *PLoS Genet.* 10:e1004170. http://dx.doi.org/10.1371/journal.pgen.1004170

Fuchs, E. 2007. Scratching the surface of skin development. *Nature.* 445:834–842. http://dx.doi.org/10.1038/nature05659

Gaiano, N., J.S. Nye, and G. Fishell. 2000. Radial glial identity is promoted by Notch1 signaling in the murine forebrain. *Neuron.* 26:395–404. http://dx.doi.org/10.1016/S0896-6273(00)81172-1

Gerdes, J.M., Y. Liu, N.A. Zaghloul, C.C. Leitch, S.S. Lawson, M. Kato, P.A. Beachy, P.L. Beales, G.N. DeMartino, S. Fisher, et al. 2007. Disruption of the basal body compromises proteasomal function and perturbs intracellular Wnt response. *Nat. Genet.* 39:1350–1360. http://dx.doi.org/10.1038/ng.2007.12

Hori, K., A. Sen, and S. Artavanis-Tsakonas. 2013. Notch signaling at a glance. *J. Cell Sci.* 126:2135–2140. http://dx.doi.org/10.1242/jcs.127308

Ishikawa, H., J. Thompson, J.R. Yates III, and W.F. Marshall. 2012. Proteomic analysis of mammalian primary cilia. *Curr. Biol.* 22:414–419. http://dx.doi.org/10.1016/j.cub.2012.01.031

Jeong, S.J., H.S. Kim, K.A. Chang, D.H. Geum, C.H. Park, J.H. Seo, J.C. Rah, J.H. Lee, S.H. Choi, S.G. Lee, et al. 2000. Subcellular localization of presenilins during mouse preimplantation development. *FASEB J.* 14:2171–2176. http://dx.doi.org/10.1096/fj.99-1068com

Jin, H., S.R. White, T. Shida, S. Schulz, M. Aguiar, S.P. Gygi, J.F. Bazan, and M.V. Nachury. 2010. The conserved Bardet-Biedl syndrome proteins assemble a coat that traffics membrane proteins to cilia. *Cell.* 141:1208–1219. http://dx.doi.org/10.1016/j.cell.2010.05.015

Kaimori, J.Y., Y. Nagasawa, L.F. Menezes, M.A. Garcia-Gonzalez, J. Deng, E. Imai, L.F. Onuchic, L.M. Guay-Woodford, and G.G. Germino. 2007. Polyductin undergoes notch-like processing and regulated release from primary cilia. *Hum. Mol. Genet.* 16:942–956. http://dx.doi.org/10.1093/hmg/ddm039

Kim, J., M. Kato, and P.A. Beachy. 2009. Gli2 trafficking links Hedgehog-dependent activation of Smoothened in the primary cilium to transcriptional activation in the nucleus. *Proc. Natl. Acad. Sci. USA.* 106:21666–21671. http://dx.doi.org/10.1073/pnas.0912180106

Kopan, R. 2012. Notch signaling. *Cold Spring Harb. Perspect. Biol.* 4:a011213. http://dx.doi.org/10.1101/cshperspect.a011213

Lechler, T., and E. Fuchs. 2007. Desmoplakin: an unexpected regulator of microtubule organization in the epidermis. *J. Cell Biol.* 176:147–154. http://dx.doi.org/10.1083/jcb.200609109

Lefort, K., and G.P. Dotto. 2004. Notch signaling in the integrated control of keratinocyte growth/differentiation and tumor suppression. *Semin. Cancer Biol.* 14:374–386. http://dx.doi.org/10.1016/j.semcancer.2004.04.017

Leitch, C.C., S. Lodh, V. Prieto-Echagüe, J.L. Badano, and N.A. Zaghloul. 2014. Basal body proteins regulate Notch signaling through endosomal trafficking. *J. Cell Sci.* 127:2407–2419. http://dx.doi.org/10.1242/jcs.130344

Litingtung, Y., R.D. Dahn, Y. Li, J.F. Fallon, and C. Chiang. 2002. Shh and Gli3 are dispensable for limb skeleton formation but regulate digit number and identity. *Nature.* 418:979–983. http://dx.doi.org/10.1038/nature01033

Mazelova, J., L. Astuto-Gribble, H. Inoue, B.M. Tam, E. Schonteich, R. Prekeris, O.L. Moritz, P.A. Randazzo, and D. Deretic. 2009. Ciliary targeting motif VxPx directs assembly of a trafficking module through Arf4. *EMBO J.* 28:183–192. http://dx.doi.org/10.1038/emboj.2008.267

Mill, P., R. Mo, M.C. Hu, L. Dagnino, N.D. Rosenblum, and C.C. Hui. 2005. Shh controls epithelial proliferation via independent pathways that converge on N-Myc. *Dev. Cell.* 9:293–303. http://dx.doi.org/10.1016/j.devcel.2005.05.009

Mizutani, K., K. Yoon, L. Dang, A. Tokunaga, and N. Gaiano. 2007. Differential Notch signalling distinguishes neural stem cells from intermediate progenitors. *Nature.* 449:351–355. http://dx.doi.org/10.1038/nature06090

Molla-Herman, A., R. Ghossoub, T. Blisnick, A. Meunier, C. Serres, F. Silbermann, C. Emmerson, K. Romeo, P. Bourdoncle, A. Schmitt, et al. 2010. The ciliary pocket: an endocytic membrane domain at the base of primary and motile cilia. *J. Cell Sci.* 123:1785–1795. http://dx.doi.org/10.1242/jcs.059519

Narita, K., H. Kozuka-Hata, Y. Nonami, H. Ao-Kondo, T. Suzuki, H. Nakamura, K. Yamakawa, M. Oyama, T. Inoue, and S. Takeda. 2012. Proteomic analysis of multiple primary cilia reveals a novel mode of ciliary development in mammals. *Biol. Open.* 1:815–825. http://dx.doi.org/10.1242/bio.20121081

Nizzari, M., V. Venezia, P. Bianchini, V. Caorsi, A. Diaspro, E. Repetto, S. Thellung, A. Corsaro, P. Carlo, G. Schettini, et al. 2007. Amyloid precursor protein and Presenilin 1 interaction studied by FRET in human H4 cells. *Ann. N. Y. Acad. Sci.* 1096:249–257. http://dx.doi.org/10.1196/annals.1397.091

Nowak, J.A., and E. Fuchs. 2009. Isolation and culture of epithelial stem cells. *Methods Mol. Biol.* 482:215–232. http://dx.doi.org/10.1007/978-1-59745-060-7_14

Oro, A.E., and K. Higgins. 2003. Hair cycle regulation of Hedgehog signal reception. *Dev. Biol.* 255:238–248. http://dx.doi.org/10.1016/S0012-1606(02)00042-8

Ouspenskaia, T., I. Matos, A.F. Mertz, V.F. Fiore, and E. Fuchs. 2016. WNT-SHH Antagonism Specifies and Expands Stem Cells prior to Niche Formation. *Cell.* 164:156–169. http://dx.doi.org/10.1016/j.cell.2015.11.058

Pan, Y., M.H. Lin, X. Tian, H.T. Cheng, T. Gridley, J. Shen, and R. Kopan. 2004. gamma-secretase functions through Notch signaling to maintain skin appendages but is not required for their patterning or initial morphogenesis. *Dev. Cell.* 7:731–743. http://dx.doi.org/10.1016/j.devcel.2004.09.014

Rangarajan, A., C. Talora, R. Okuyama, M. Nicolas, C. Mammucari, H. Oh, J.C. Aster, S. Krishna, D. Metzger, P. Chambon, et al. 2001. Notch signaling is a direct determinant of keratinocyte growth arrest and entry into differentiation. *EMBO J.* 20:3427–3436. http://dx.doi.org/10.1093/emboj/20.13.3427

Rohatgi, R., L. Milenkovic, and M.P. Scott. 2007. Patched1 regulates hedgehog signaling at the primary cilium. *Science.* 317:372–376. http://dx.doi.org/10.1126/science.1139740

Rustighi, A., L. Tiberi, A. Soldano, M. Napoli, P. Nuciforo, A. Rosato, F. Kaplan, A. Capobianco, S. Pece, P.P. Di Fiore, and G. Del Sal. 2009. The prolyl-isomerase Pin1 is a Notch1 target that enhances Notch1 activation in cancer. *Nat. Cell Biol.* 11:133–142. http://dx.doi.org/10.1038/ncb1822

Satir, P., and S.T. Christensen. 2007. Overview of structure and function of mammalian cilia. *Annu. Rev. Physiol.* 69:377–400. http://dx.doi.org/10.1146/annurev.physiol.69.040705.141236

Ward, H.H., U. Brown-Glaberman, J. Wang, Y. Morita, S.L. Alper, E.J. Bedrick, V.H. Gattone II, D. Deretic, and A. Wandinger-Ness. 2011. A conserved signal and GTPase complex are required for the ciliary transport of polycystin-1. *Mol. Biol. Cell.* 22:3289–3305. http://dx.doi.org/10.1091/mbc.E11-01-0082

Watt, F.M. 2002. The stem cell compartment in human interfollicular epidermis. *J. Dermatol. Sci.* 28:173–180. http://dx.doi.org/10.1016/S0923-1811(02)00003-8

Williams, S.E., S. Beronja, H.A. Pasolli, and E. Fuchs. 2011. Asymmetric cell divisions promote Notch-dependent epidermal differentiation. *Nature.* 470:353–358. http://dx.doi.org/10.1038/nature09793

Wood, C.R., K. Huang, D.R. Diener, and J.L. Rosenbaum. 2013. The cilium secretes bioactive ectosomes. *Curr. Biol.* 23:906–911. http://dx.doi.org/10.1016/j.cub.2013.04.019

Zhang, Q., J. Hu, and K. Ling. 2013. Molecular views of Arf-like small GTPases in cilia and ciliopathies. *Exp. Cell Res.* 319:2316–2322. http://dx.doi.org/10.1016/j.yexcr.2013.03.024